

ԵՐԵՎԱՆԻ ՖԻԶԻԿԱԿԱՆ ԻՆՏԻՏՈՒՏ  
ЕРЕВАНСКИЙ ФИЗИЧЕСКИЙ ИНСТИТУТ

ЕФИ-334(59)-78

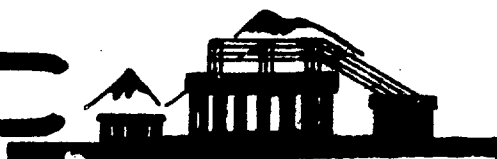
ՏՆԿՈՒԹՅՈՒՆ

S.M.DARBINIAN, K.A.ISPIRIAN

ANGULAR DISTRIBUTION AND POLARIZATION OF  
ELECTRON BREMSSTRAHLUNG IN CRYSTAL

ԱՐՄՍ

ԵՐԵՎԱՆ



ЕРЕВАН

ЕФИ-334(59)-78

**С.М.ДАРЕБИЯН, К.А.ИСПИРЯН**  
**УГЛОВОЕ РАСПРЕДЕЛЕНИЕ И ПОЛЯРИЗАЦИЯ**  
**КОГЕРЕНТНОГО ТОРМОЗНОГО ИЗЛУЧЕНИЯ**

Исследована зависимость интенсивности и поляризации когерентного тормозного излучения электронов высоких энергий в кристалле от полярного и азимутального углов испущенных фотонов. Показано, что угловое распределение тормозного излучения в кристалле сильно отличается от углового распределения в аморфных средах.

Ереванский физический институт  
Ереван 1978

ЕФМ-334(59)-78

S.M. DARBINIAN, K.A. ISPIRIAN

ANGULAR DISTRIBUTION AND POLARIZATION  
OF ELECTRON BREMSSTRAHLUNG IN CRYSTAL

The polar and azimuthal angle dependence of the intensity and polarization of high energy electron coherent radiation in crystals is investigated. It is shown that the angular distribution of the bremsstrahlung in crystal differs strongly from that for amorphous media.

Yerevan Physics Institute

Yerevan 1978

YEREVAN PHYSICS INSTITUTE

ЭИИ-334(59)-78

S.M. DARBINIAN, K.A. ISPIRIAN

ANGULAR DISTRIBUTION AND POLARIZATION  
OF ELECTRON BREMSSTRAHLUNG IN CRYSTAL

Yerevan 1978

© *Ереванский физический институт, 1978*

## 1. Introduction

At present the quasimonochromatic and polarized photon beams produced by high energy electrons passing through crystalline targets have found a wide application in elementary particle photoproduction experiments. In this connection it is of great interest to carry out detailed investigation of the production mechanism of the coherent bremsstrahlung in order to improve the characteristics of such beams.

Still in the work [1] it has been mentioned that the polarization and monochromatic characteristics for the photon beams emitted in certain narrow angular intervals are better than for beams emitted in the whole radiation cone. Then the angular distribution and polarization of the coherent bremsstrahlung have been investigated by the pseudophoton method in [2]. The same problems have been considered in [3-5] taking into account the crystal structure more accurately. In particular in the work [3] it has been shown that the polar angle,  $\theta_1$ ,

dependence of the radiation intensity for certain photon energies (after integration over the azimuthal angles,  $\varphi_1$ ) has sharp peaks at certain values of  $\theta_1$ , while the spectral distribution of the radiation emitted in a narrow interval  $\Delta\theta_1$  differs from that of emitted in the whole radiation cone and has a high monochromaticity. In [4] it is given the radiation spectra and the results of polarization calculations for the case of very narrow axial collimation taking into account the angular divergence and multiple scattering of the electron beam. Finally, in [5] the azimuthal angle dependence of the radiation emitted in certain polar angle interval  $\Delta\theta_1$  is investigated and it is shown that the beam polarization increases significantly for the case of nonaxial collimation.

The experimental investigation of the polar and azimuthal angle dependence of the coherent bremsstrahlung is a difficult problem not only for the smallness of the radiation cone but also due to the multiple scattering and angular divergence of the primary electron beam. Nevertheless such experiments have already begun [6]. On the other hand the knowledge of the angular dependences is necessary for the calculation of the high energy photon beam polarization since usually the degree of polarization is computed using the experimentally measured spectral distribution. For instance in the work [7] in which a Monte Carlo method for polarization calculation is developed it is assumed that the coherent part of the radiation just as the incoherent part has a Gauss polar angle distribution and does not depend on the azimuthal angle.

The aim of the present work is to derive of the expres -

sions for the cross sections and polarization differential with respect to the both polar and azimuthal angles to carry out numerical calculation on the angular distributions of coherent bremsstrahlung.

## 2. Kinematics

The energy and momentum conservation laws for the process of bremsstrahlung on nucleus have the form :

$$\begin{aligned} \varepsilon_1 &= \varepsilon_2 + \omega, \\ \vec{P}_1 &= \vec{P}_2 + \vec{K} + \vec{q}, \end{aligned} \quad (1)$$

where  $\vec{P}_1, \varepsilon_1; \vec{P}_2, \varepsilon_2; \vec{K}, \omega$  are the momenta and energies of the primary, final electrons and photons, respectively,  $\vec{q}$  is the momentum transferred to the nucleus ( $\hbar = c = m = 1$ ). Coming out from (1) in the high energy and small angle approximation one obtains the following relation between the parallel,  $q_{\parallel}$ , and perpendicular,  $q_{\perp}$ , components of  $\vec{q}$  with respect to  $\vec{P}_1$  :

$$q_{\parallel} - \delta \cdot (1 + u^2) - q_{\perp}^2 / 2\varepsilon_2 - 2\delta \cdot u q_{\perp} \cos(\varphi_1 - \varphi_q) = 0. \quad (2)$$

Here  $\delta = \omega / 2\varepsilon_1\varepsilon_2$  is the minimal momentum transfer,  $u = \varepsilon_1 \theta_1$  is the photon emission angle,  $\varphi_1$  and  $\varphi_q$  are the azimuthal angle of the photon and momentum transfer, respectively. For the interference part of the radiation one has  $\vec{q} = \vec{g}$  where  $\vec{g}$  is the reciprocal lattice vector. The

direction of the primary electron motion (along  $Z$ -axis) is defined by the entrance angles  $\theta$  and  $\alpha$  with respect to the crystal axes  $b_1$ ,  $b_2$  and  $b_3$  (see Fig.1). Then for small angles  $\theta$  one may write the following relations for the parallel,  $g_{||}$ , and perpendicular,  $g_{\perp}$ , components of the vector  $\vec{g}$  :

$$g_{||} = g_3 + \theta (g_1 \sin \alpha - g_2 \cos \alpha),$$

$$g_x = g_1 \cos \alpha + g_2 \sin \alpha, \quad (3)$$

$$g_y = -g_1 \sin \alpha + g_2 \cos \alpha,$$

where  $g_1$ ,  $g_2$  and  $g_3$  are the components of  $\vec{g}$  along the crystallographic axes  $b_1$ ,  $b_2$  and  $b_3$ .

For the given values  $u$  and  $\varphi_1$  equation (2) represents the known paraboloid in  $\vec{q}(\vec{g})$ -space, while for a given reciprocal lattice vector  $\vec{g}$  equation (2) is a circle with respect to the variables  $u_x = -u \cos \varphi_1$  and  $u_y = -u \sin \varphi_1$ .

$$(u_x - g_x)^2 + (u_y - g_y)^2 = \frac{1}{\delta} (g_{||} - \delta - g_{\perp}^2 / 2\varepsilon_1). \quad (4)$$

For the given  $\vec{g}$  and certain values of  $\varepsilon_1$  and  $\chi = \omega / \varepsilon_1$  equation (4) connects the values of the angles  $u$  and  $\varphi_1$  with each other. The possible values of the azimuthal angle  $\varphi_1$  under which the emission of photon with polar angle  $u$  takes place are determined by the crossing point of the circle (4) with the circle  $u = \text{const}$  and one may obtain them solving eq.(4) with respect to  $\varphi_1$  :

$$\left. \begin{aligned} \varphi_1^{(1)} &= \psi_1 + \psi_2, \\ \varphi_1^{(2)} &= \psi_1 - \psi_2 \end{aligned} \right\} \text{ for } g_y > 0, \quad (5)$$

$$\left. \begin{aligned} \varphi_1^{(1)} &= -\psi_1 + \psi_2, \\ \varphi_1^{(2)} &= -\psi_1 - \psi_2 \end{aligned} \right\} \text{ for } g_y < 0,$$

where

$$\psi_1 = \arccos(g_x/g_y),$$

$$\psi_2 = \arccos\left[\frac{g_{||}}{\delta} - 1 - u^2 - g_{\perp}^2/x\right] / 2ug \quad (5')$$

Since  $\varphi_1$  varies in the limits  $0 \div 2\pi$  then it is necessary to add  $2\pi$  to the negative values of  $\varphi_1$ .

Eq.(4) determines also the angular interval  $u_{\min} \leq u \leq u_{\max}$  into which the given reciprocal lattice vector gives contribution:

$$u_{\min}^{\max} = \left| g_{\perp} \pm \sqrt{(g_{||} - \delta - g_{\perp}^2/2\varepsilon_1)/\delta} \right|. \quad (6)$$

If in the right hand side of eq. (2) one neglects the second and third terms proportional to the small magnitude  $g_{\perp}$  and its square then eq. (4) takes the form  $u^2 = (g_{||} - \delta)/\delta$ , and in this case there is no dependence of  $u$  on  $\varphi_1$ . Therefore we shall not neglect these terms for a more correct analysis of the radiation angular characteristics.

For illustration let us consider eq.(4) in more detail for a particular case of diamond crystal orientation when  $\mathcal{C}_1 = [001]$ ,  $\mathcal{C}_2 = [1\bar{1}0]$ ,  $\mathcal{C}_3 = [110]$ . In this case:

$$g_{11} = \frac{2\pi}{a} \theta \left( n_1 \sin \alpha - n_2 \sqrt{2} \cos \alpha \right),$$

$$g_{12} = \frac{2\pi}{a} \left( n_1 \cos \alpha + n_2 \sqrt{2} \sin \alpha \right), \quad (7)$$

$$g_{22} = \frac{2\pi}{a} \left( -n_1 \sin \alpha + n_2 \sqrt{2} \cos \alpha \right),$$

where  $a$  is the lattice constant,  $n_1$ ,  $n_2$  are integral numbers. In Fig.2 the circles (4) are shown in the plane  $U_x, U_y$  for electrons with energy  $E_1 = 1$  GeV and two values of  $\chi = \omega/E_1$ . The figure reminds diffraction pattern. For the given case the numbers of the bands are determined by the value of  $n_2$ . For the given  $\chi$  the minimal and maximal values of  $U$  (The circles 1,1'; 2,2'; 3,3' in Fig.2) are determined by the maximal values of  $n_1$  up to which the calculations are carried out. It is necessary to note that the intensity decreases sharply when in the given band ( $n_2 = \text{const}$ ) one increases the values of  $n_1$ .

In Fig.3 the circles (4) are shown in the plane  $U_x, U_y$  for electrons with energy  $E = 1$  GeV, for three values of  $\chi$  for the case when crystal orientation is chosen in such a way that mainly one reciprocal lattice vector (220) gives contribution. The contribution of other ones into the intensity is negligible. The boundary circles 1,1'; 2,2'; 3,3' correspond to the minimal and maximal values of  $U$  in the limits of which the coherent radiation dominates.

Thus, the kinematics taking into account the small terms allows to establish the discrete character of the coherent

radiation angular distribution and determine the angular interval  $\Delta U$  into which the emission of coherent photons takes place for the given  $E_1, \chi, \theta$  and  $\lambda$ .

### 3. Differential Cross Sections and Polarization

Let us obtain the cross section for bremsstrahlung in crystal, differential with respect to the energy and angles of the emitted photon, as well as the photon Stokes parameters. The calculations are carried out in the Born approximation with exponential screening of the nucleus field by atomic electrons. The initial electron is assumed to be polarized while a summation over the polarization of the final electron is carried out. We come out from the expression for the differential cross section on single atom given in the form [9,10]:

$$d^b\sigma = \sigma_0 \frac{2}{\pi^2} \frac{1}{(q^2 + \beta^2)^2} |\vec{A}\vec{e}^*|^2 \delta(\varepsilon_1 - \varepsilon_2 - \omega) \frac{d\omega}{\omega} d\Omega_1 d\vec{p}_2, \quad (8)$$

where  $\sigma_0 = Z^2 r_0^2 / 137$ ,  $r_0 = e^2 / mc^2$ ,  $d\Omega_1 = \theta_1 d\theta_1 d\varphi_1$ ,  $\beta = Z / 111$ ,  $\vec{e}$  is a unit polarization vector of photon,

$$|\vec{A}\vec{e}^*|^2 = \frac{1}{2} \omega^2 \vec{J}^2 + 2\varepsilon_1 \varepsilon_2 |\vec{J}\vec{e}|^2 + \quad (9)$$

$$+ \frac{\omega}{2} (\varepsilon_1 + \varepsilon_2) \vec{J}^2 (\vec{\delta}_1 [i\vec{e} \times \vec{e}^*]) - \omega \varepsilon_2 (\vec{J}\vec{\delta}) (\vec{J} [i\vec{e} \times \vec{e}^*]),$$

$$\vec{J} = \beta \vec{U} - \eta \vec{V} - \hat{K} (\beta - \eta). \quad (10)$$

Here  $\vec{P}_1$  is the primary electron polarization,

$$\vec{u} = \vec{P}_1 - (\vec{P}_1 \hat{R}) \hat{R}, \quad \vec{v} = \vec{P}_2 - (\vec{P}_2 \hat{R}) \hat{R},$$

$$\xi = 1/(1+u^2), \quad \eta = 1/(1+v^2).$$

In the Born approximation one obtains the bremsstrahlung cross section in crystal multiplying (8) by the diffraction factor and averaging over thermal oscillations of atoms [11]. As a result the cross section may be represented as a sum of the incoherent and coherent cross sections:

$$d^6\sigma^{\text{inc}} = N\sigma_0 \frac{2}{\pi^2} \frac{1 - \exp(-q^2 \bar{u}^2)}{(q^2 + \beta^2)^2} |\vec{A} \vec{e}^*|^2 \delta(\varepsilon_1 - \varepsilon_2 - \omega) \frac{d\omega}{\omega} d\Omega_1 d\vec{P}_2, \quad (11)$$

$$d^6\sigma^{\text{coh}} = N\sigma_0 \frac{2}{\pi^2} \frac{1 - \exp(-q^2 \bar{u}^2)}{(q^2 + \beta^2)^2} |\vec{A} \vec{e}^*|^2 \cdot$$

$$\cdot \sum_{\vec{g}} \frac{(2\pi)^3}{V_0} \frac{S(\vec{g})}{n_0} \delta(\vec{q} - \vec{g}) \delta(\varepsilon_1 - \varepsilon_2 - \omega) \frac{d\omega}{\omega} d\Omega_1 d\vec{P}_2, \quad (12)$$

where  $\bar{u}^2$  is the mean square thermal displacement of the lattice atoms,  $S(\vec{g})$  is the crystal structure factor,  $V_0$ ,  $n_0$  are the volume and number of atoms of elementary cell,  $N$  is the number of atoms in crystal.

Let us carry out integration over  $\vec{P}_2$  in (11) and (12). For the incoherent part of the cross section this integration is carried out just as for single atom (see [9, 10]).

$$\begin{aligned}
d^3 \sigma_{\text{coh}}^{\text{inc}}(\vec{p}_2, \vec{\Sigma}_1, \vec{K}, \vec{e}) = & N \sigma_0 \frac{d\omega}{\omega} \frac{d\zeta}{\xi_1^2} \frac{d\varphi_1}{2\pi} \left\{ (\xi_1^2 + \xi_2^2) [\beta + 2\Gamma(\zeta)] - \right. \\
& - 2\xi_1 \xi_2 - 16\xi_1 \xi_2 \zeta^2 \Gamma(\zeta) |\vec{u}\vec{e}|^2 + \\
& + [\omega(\xi_1 + \xi_2)(\beta + 2\Gamma) + 2\omega\xi_2(1 + 4u^2 \zeta^2 \Gamma)] (\vec{\Sigma}_1 \vec{K}) (\hat{K} [i\vec{e} * \vec{e}^*])^{(13)} \\
& \left. - 4\omega\xi_2 \zeta (2\zeta - 1) \Gamma(\zeta) (\vec{\Sigma}_1 \vec{u}) (\hat{K} [i\vec{e} * \vec{e}^*]) \right\}.
\end{aligned}$$

This expression coincides with the formula (7.1) of the work [3]. In the case of exponential screening with a good accuracy we have:

$$\Gamma(\zeta) = -2 - \ln(\beta\zeta) - \frac{1}{4} B(\beta^2 u^2), \quad (14)$$

where  $B(x)$  is a known function [11] the numerical value of which  $B(\beta^2 u^2) = 4.44$  for diamond at  $T = 300^\circ\text{K}$ .

In order to integrate the coherent part of the cross section (12) over  $\vec{p}_2$  it is suitable to change the variable  $\vec{p}_2 = \vec{p}_1 - \vec{K} - \vec{q}$  and then carry out integration over  $\vec{q}$ . Due to the presence of the delta function  $\delta(\vec{q} - \vec{g})$  the integration over  $\vec{q}$  is replaced by a summing over  $\vec{g}$ . Omitting the detailed calculations one may represent the result in the following form:

$$d\sigma_{\text{coh}}^{\text{inc}}(\vec{p}_1, \vec{\Sigma}_1, \vec{K}, \vec{e}) = 4N\sigma_0 \frac{d\omega}{\omega} \frac{d\Omega_1}{\pi} \sum_{\vec{g}} B(\vec{g}) |\vec{A}\vec{e}^*|^2 \delta\{\phi(\vec{K}, \vec{g})\}, \quad (15)$$

where

$$D(g) = \frac{(2\pi)^2}{V_0} \frac{S(g)}{n_0} \frac{\exp(-g^2 \bar{u}^2)}{(g^2 + \beta^2)^2},$$

$|\vec{A} \vec{e}^*|^2$  has the form of (9), however, now

$$J^2 = \int \eta g_{\perp}^2, \quad \eta = \frac{\delta}{g_{\parallel} - g_{\perp}^2 / 2\varepsilon_1}, \quad \vec{V} = \vec{u} - \vec{g}. \quad (16)$$

The argument of the  $\delta$ -function is the left hand side of eq.(2) with the replacement of  $\vec{q}$  by  $\vec{g}$ . The limits of summation over  $\vec{g}$  in (15) are determined by the equation  $\phi(\vec{K}, \vec{g}) = 0$ .

The formulae (13), (15) allow to calculate the main characteristics of the electron bremsstrahlung in crystal. Carrying out the summation over the photon polarizations we obtain bremsstrahlung angular distribution  $d^3\sigma(\vec{P}_1, \vec{K})$ . To obtain the degree of polarization  $P$  we calculate the Stockes parameters  $\xi_1, \xi_2, \xi_3$  choosing the main oris in the plane  $(\vec{P}_1, \vec{e}_3)$  and perpendicularly to this plane (see Fig.1). Let us note, that the Stockes parameter  $\xi_3$  corresponds to the photon linear polarization in the plane  $(\vec{P}_1, \vec{e}_3)$  while  $\xi_1$  corresponds to the linear polarization along a direction making  $45^\circ$  to the plane  $(\vec{P}_1, \vec{e}_3)$ .  $\xi_2^{(||)}$  and  $\xi_2^{(\perp)}$  are the circular photon polarizations from longitudinally ( $\hat{P}_1 \hat{\xi}_2 = \pm 1$ ) and transversally ( $\hat{P}_1 \hat{\xi}_2 = 0$ ) polarized electrons. Since in general case the direction of maximal linear polarization may differ from the chosen directions for  $\xi_3$  and  $\xi_1$  then the degree of linear

polarization and the angle  $\Psi$  between the plane of maximal polarization and the plane  $(\vec{P}_1, \vec{b}_3)$  are determined by the expressions:

$$P = \sqrt{\beta_1^2 + \beta_3^2}, \quad \operatorname{tg} 2\Psi = \beta_1 / \beta_3. \quad (17)$$

Omitting the detailed calculations let us give the expressions for the radiation angular distribution as well as for Stokes parameters in the following standart form:

$$d^3\sigma^{(0)}(\vec{P}_1, \vec{K}) = N\sigma_0 \frac{d\omega}{\omega} \frac{d\Omega^2 d\varphi_1}{2\pi} I(\vec{P}_1, \vec{K}), \quad (18)$$

$$\beta_3(\vec{P}_1, \vec{K}) = 2(1-x)(\phi_3^a + \phi_3^i) / I(\vec{P}_1, \vec{K}), \quad (19)$$

$$\beta_1(\vec{P}_1, \vec{K}) = 2(1-x)(\phi_4^a + \phi_4^i) / I(\vec{P}_1, \vec{K}), \quad (20)$$

$$\beta_2^{(II)}(\vec{P}_1, \vec{K}) = \pm [x(2-x)(\phi_1^a + \phi_1^i) - \frac{2}{3}x(1-x)(\phi_2^a + \phi_2^i)] / I(\vec{P}_1, \vec{K}), \quad (21)$$

$$\beta_2^{(I)}(\vec{P}_1, \vec{K}) = -8x(1-x)(\phi_5^a + \phi_5^i) / I(\vec{P}_1, \vec{K}), \quad (22)$$

where

$$I(\vec{P}_1, \vec{K}) = [1 + (1-x)^2](\phi_1^a + \phi_1^i) - \frac{2}{3}(1-x)(\phi_2^a + \phi_2^i), \quad (23)$$

$$\phi_1^a = 2 \xi^2 [3 + 2 \Gamma(\frac{3}{2})],$$

$$\phi_2^a = 6 \xi^2 [1 + 4 u^2 \xi^2 \Gamma(\frac{3}{2})],$$

$$\phi_3^a = 8 u^2 \xi^4 \Gamma(\frac{3}{2}) \cos 2 \varphi_1,$$

$$\phi_4^a = 8 u^2 \xi^4 \Gamma(\frac{3}{2}) \sin 2 \varphi_1,$$

$$\phi_5^a = \xi^3 (2 \xi - 1) \Gamma(\frac{3}{2}) (\vec{\xi}_1 \vec{u}),$$

$$\phi_1^i = 4 \sum_{\vec{g}} \mathcal{D}(\vec{g}) \xi \eta g_{\perp}^2 \delta\{\phi(\vec{R}, \vec{g})\}, \quad (24)$$

$$\phi_2^i = 12 \sum_{\vec{g}} \mathcal{D}(\vec{g}) (\xi - \eta)^2 \delta\{\phi(\vec{R}, \vec{g})\},$$

$$\phi_3^i = 4 \sum_{\vec{g}} \mathcal{D}(\vec{g}) [-(\xi - \eta)^2 u^2 \cos 2 \varphi_1 - \eta^2 g_{\perp}^2 \cos 2 \varphi_g + 2 \eta (\xi - \eta) u g_{\perp} \cos(\varphi_1 + \varphi_g)] \delta\{\phi(\vec{R}, \vec{g})\},$$

$$\phi_4^i = 4 \sum_{\vec{g}} \mathcal{D}(\vec{g}) [-(\xi - \eta)^2 u^2 \sin 2 \varphi_1 - \eta^2 g_{\perp}^2 \sin 2 \varphi_g + 2 \eta (\xi - \eta) u g_{\perp} \sin(\varphi_1 + \varphi_g)] \delta\{\phi(\vec{R}, \vec{g})\},$$

$$\phi_5^i = \sum_{\vec{g}} \mathcal{D}(\vec{g}) (\eta - \xi) [(\xi - \eta) (\vec{u} \vec{\xi}_1) + \eta (\vec{g}_{\perp} \vec{\xi}_1)] \delta\{\phi(\vec{R}, \vec{g})\}.$$

The expressions (18-24) are the basic formulae for calculating the angular distribution and polarization of the radiation emitted in certain solid angle as for axial as well as nonaxial collimations. They are equivalent to the corresponding differential expressions obtained for amorphous media in [9].

The expression for the cross section (18) differential with respect to  $u$  and  $\varphi_1$  was given by us in the work [13]. After simple transformations the formulae (18) and (19) come to the corresponding formulae (6-9) of the work [4]. Integrating (15) in the interval  $u, u + \Delta u$  one may obtain the  $\varphi$  - dependence and polarization of bremsstrahlung in crystal which are studied in [5]. Finally, the integration of the corresponding expressions (15-23) over the angles results in the well known formula for the spectrum and polarization of bremsstrahlung in crystal [8,11,12]:

It is necessary to note that the presence of  $\delta$  -function in the differential expressions for coherent bremsstrahlung makes difficult the analysis of the angular distributions and for this reason in the works devoted to the coherent bremsstrahlung usually the  $\delta$  -functions do not manifest themselves after carrying out integration in certain angular intervals. The formulae (15-24) allow to obtain not only the known results [4,5,8,11,12] but also the unstudied characteristics of coherent bremsstrahlung, for instance, the radiation polar angle distribution (see below).

#### 4. Results and Discussion

The main advantage of writing the radiation formulae in the form (18-24) is in the possibility to determine the azimuthal angle of the emitted coherent photon for the given  $u$  and  $\vec{g}$ . To obtain the  $u$  and  $\varphi$  - dependences as well as the polarization of the radiation let us represent the  $\delta$  - function in (24) in the following form:

$$\delta[a - b \cos(\varphi_1 - \varphi_2)] = \frac{1}{\sqrt{a^2 - b^2}} \sum_{i=1}^2 \delta(\varphi_1 - \varphi_1^{(i)}), \quad (25)$$

where  $a$  and  $b$  are determined from the  $\delta$ -function argument:

$$\begin{aligned} a &= g_{\parallel} - \delta - \delta u^2 - g_{\perp}^2 / 2\epsilon_2, \\ b &= 2\delta u g_{\perp}, \end{aligned} \quad (26)$$

and  $\varphi_1^{(i)}$  are given by the formulae (5).

In our numerical calculations we formally carry out integration of (18-24) over  $\varphi_1$  using the expression (25), however, during the summation over the reciprocal lattice vector  $\vec{g}$  each time we fix the value of azimuthal angle for the given  $u$ . Let us note that the limits of summation over  $\vec{g}$  are determined by the condition that the expression under square root in (25) is to be positive. Thus giving the values of the parameters  $E, x, \theta, L$  we obtain the radiation  $u$  and  $\varphi$  - dependences.

In Fig 4a it is given the dependence of the radiation intensity  $I$  on the polar angle  $U$  after integration over  $\varphi_1$  for electrons with energy  $E = 1$  GeV passing through diamond. The coherent radiation intensities (curves 1,2,3) at  $\chi = 0.29$ ; 0.25; 0.2 are given only in that  $U$  intervals in which they dominate over the noncoherent radiation intensity (curve 4, which is almost independent of  $\chi$  for this case). The radiation intensity integrated over all the angles has maximum at  $\chi_d = 0.3$  (see Fig.18b of the work [8]).

As it is seen from Fig.4a the essential difference between the coherent and incoherent radiation intensities is in the fact that for the given value of  $\chi$  the coherent intensity is higher than the incoherent one more than some order only in certain narrow angular intervals  $\Delta U$ . For the given  $E, \chi, \theta, \lambda$  there is a minimal value of  $U$  below which there is no coherent radiation. The regions  $\Delta U$  in Fig. 4a correspond to the bands in Fig.2. Let us, however, note that as it is expected the coherent radiation intensity integrated over all  $U$  is only some times higher than the corresponding incoherent intensity.

In Fig.4b it is given the dependence of the radiation polarization  $P$  upon  $U$  after integration over  $\varphi_1$ . As it was expected the degree of polarization for  $\chi = 0.29$  (closer to  $\chi_d$ ) is higher than for  $\chi = 0.25$  and  $\chi = 0.2$ .

The  $U$  - dependences of the radiation intensity and polarization for "one point" effect when the contribution of the reciprocal lattice vector (220) dominates (the parameters are the same as in Fig.3) are shown in Fig.5a and b, respectively.

vely for  $\chi = 0.29$  (curve 1),  $\chi = 0.25$  (curve 2) and  $\chi = 0.21$  (curve 3). As it is seen from Figs 4b and 5b in spite of the case when many reciprocal lattice vectors give contribution in the case of "one point" effect there is no narrow dip in the polarization curves at values of  $U$  corresponding to the intensity maxima.

To obtain the azimuthal angle,  $\varphi_1$ , dependence of the radiation intensity we carry out computer numerical integration of (18-24) over  $U$  in certain intervals  $\Delta U$ . In principle one may carry out such an integration for any interval  $\Delta U$ , however, to obtain stronger  $\varphi_1$  dependence and higher degree of polarization it is natural to carry out integration in that intervals  $\Delta U$  where contribution of the coherent radiation dominates significantly over that of incoherent radiation (see Figs 4a and 5a).

As it has been mentioned above for each value of  $U$  the computer gives certain values of  $\varphi_1$ . For the below given results the whole interval of  $\varphi_1$  from 0 up to  $2\pi$  we have in particular divided into 12 equal intervals. Thus, the computer provides the intensity, Stockes parameters  $\xi_1$  and  $\xi_3$ , polarization  $P$  and angle  $\psi$  for radiation emitted into 12 solid angles equal each to other and defined by  $\Delta U = U_{\max} - U_{\min}$  and  $\Delta\varphi_1 = \pi/6$

In Fig. 6a and b it is given the azimuthal angle  $\varphi_1$  dependence of the intensity  $I$  and corresponding polarization  $P$

for electrons and crystal with same values of parameters as in Fig.2 and 4. As it is seen from Fig.6a in the case when many reciprocal lattice vectors give contribution the azimuthal dependence of the radiation intensity is weaker for  $\chi = 0.29$  (histogram 1) than for  $\chi = 0.25$  and  $\chi = 0.21$  (histograms 2 and 3). Though the degrees of polarization (Fig.6b) for  $\chi = 0.29$  (histogram 1) is less than for  $\chi = 0.25$  and  $\chi = 0.2$  (histograms 2 and 3), nevertheless, as it was expected the integrated over all the possible  $\psi_1$  degree of polarization is higher for  $\chi = 0.29$  than for  $\chi = 0.25$  and  $\chi = 0.2$ . This is a consequence of the fact that when  $\psi_1$  varies in the interval  $0 \div 2\pi$  the angle  $\psi$  changes its sign more frequently in the cases of the histograms 2 and 3 than for the case of histogram 1. The values of degree of polarization after integration of all  $\psi_1$  are 0.38; 0.35 and 0.25 for the histograms 1, 2 and 3, respectively. Such behaviour for azimuthal angle dependence of radiation intensity and polarization is obtained also for "one point" effect.

Thus, the calculations carried out by the method and formulae developed in this work show that the polar angle dependence of the coherent bremsstrahlung differs strongly from the corresponding dependence of the incoherent radiation. The study of the azimuthal angle dependence confirms the fact that in principle one may improve the characteristics of photon beams by a proper non axial collimation.

The authors thank N.Z.Akopov for help during the numerical calculations and discussion.

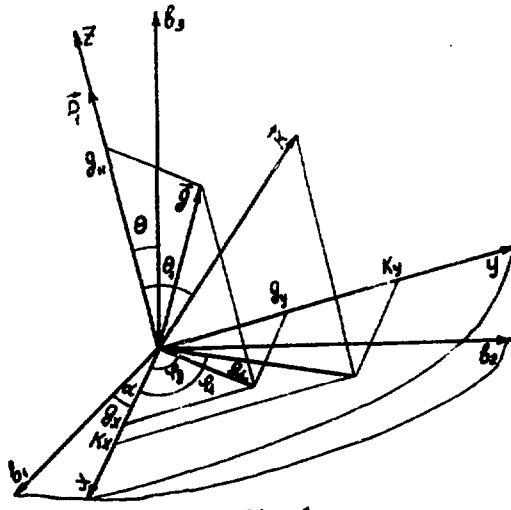


Fig. 1.

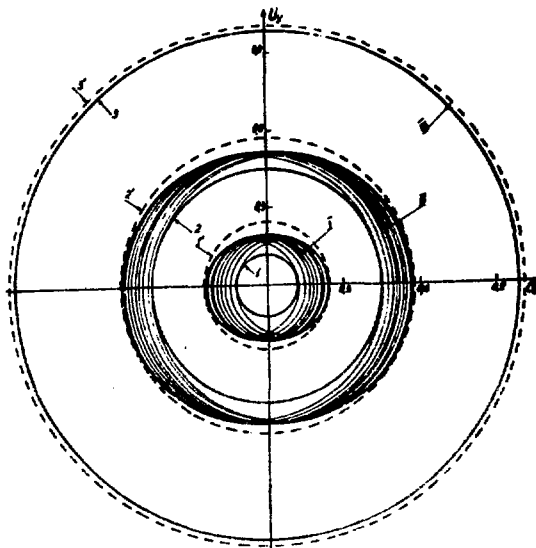


Fig. 2

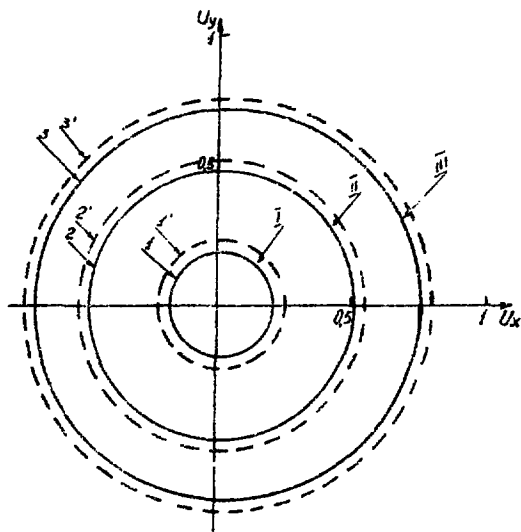


Fig. 3

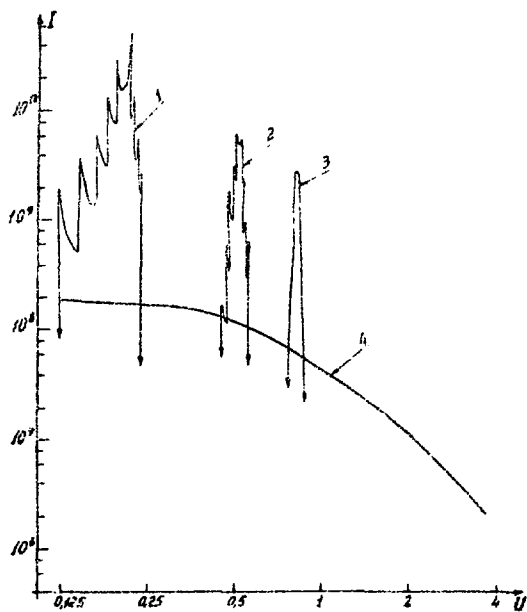


Fig. 4a

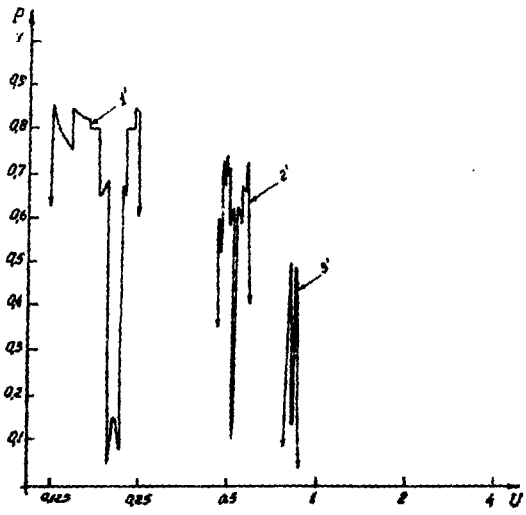


Fig.4b

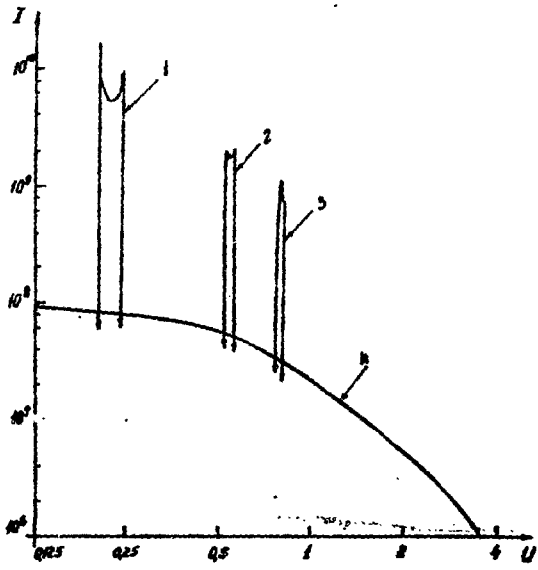


Fig.5a

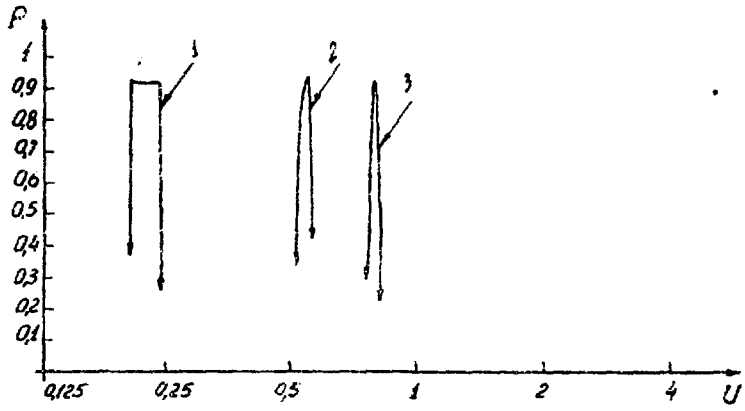


Fig. 5b

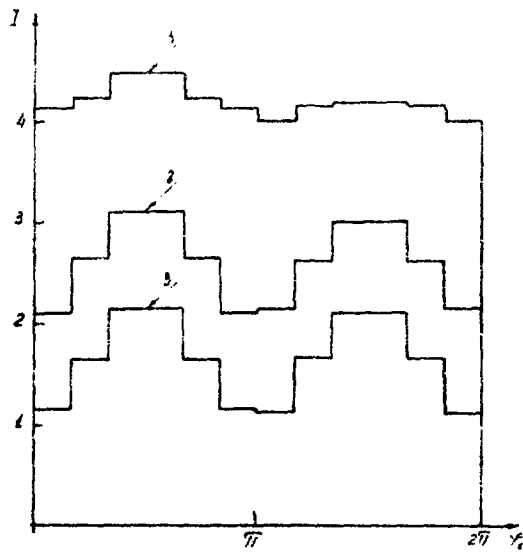


Fig. 5a

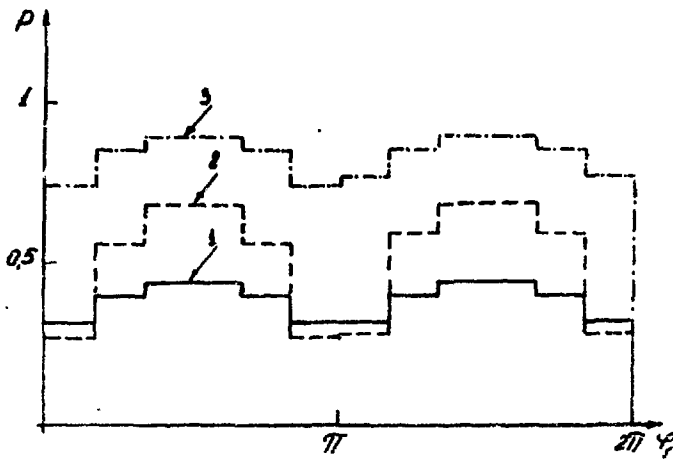


Fig.6b

Figure Captions

Fig. 1. Orientation of the coordinate frame  $x, y, z$  relative to the crystallographic axes  $b_1, b_2, b_3$ .

Fig. 2. Diagrams  $U = U(\varphi)$  at various  $\vec{g}$  for electrons with energy  $E = 1$  GeV in diamond. The direction of the electron entrance into the crystal is chosen so that  $\theta = 11,3$  mrad,  $\alpha = 0$ ,  $b_1 = [001]$ ,  $b_2 = [1\bar{1}0]$ ,  $b_3 = [110]$ .

Bands I -  $\chi = 0.29$ ;  $n_2 = -1$ ;  $n_1 = \pm 1 \dots \pm 9$ ;

II -  $\chi = 0.25$ ;  $n_2 = -1$ ;  $n_1 = \pm 1 \dots \pm 9$ ;

III -  $\chi = 0.2$ ;  $n_2 = -2$ ;  $n_1 = 0, \pm 4, \pm 8$ .

Fig. 3. Diagrams  $U = U(\varphi)$  for the reciprocal lattice vector (220) for electrons with  $E = 1$  GeV in diamond. The direction of the electron entrance into the crystal is chosen so that  $\theta = 50$  mrad;  $\alpha = 0.899$  rad,  $b_1 = [100]$ ,  $b_2 = [010]$ ,  $b_3 = [001]$  ("one point" effect). The bands I, II and III are for  $\chi = 0.29$ ; 0.25 and 0.21, respectively.

Fig. 4a. Dependence of the intensity  $I = (\chi/2\pi N\sigma_c) d^2\sigma/dx d\theta_1 d\theta_2$  on  $U$ . The curves 1, 2, 3 are for coherent radiation with  $\chi = 0.29$ ; 0.25 and 0.2, respectively. The curve 4 is for incoherent radiation. The parameters of the electrons and crystal are the same as in Fig. 2.

Fig. 4b. Dependence of the polarization  $P$  on  $U$  for the case of Fig. 4a.

Fig. 5a. Dependence of the intensity  $I = (\chi/2\pi N\sigma_c) d^2\sigma/dx d\theta_1 d\theta_2$

on  $U$ . The curves 1,2,3 are for coherent radiation for  $\chi = 0.29, 0.25$  and  $0.21$ , respectively. The curve 4 is for incoherent radiation. The parameters are the same as in Fig.3.

Fig.5b. Dependence of the polarization  $P$  on  $U$  for the case of Fig.5a.

Fig.6a. Dependence of the intensity  $I = \frac{\chi}{N\sigma_0} \int_{u_1}^{u_2} \int_{\varphi_1}^{\varphi_2} \frac{d^3\sigma}{dx du^2 d\varphi_1} du^2 d\varphi_1$  on  $\varphi_1$ . The histograms 1,2,3 are for  $\chi = 0.29, 0.25$  and  $0.2$ , respectively. The parameters are the same as in Fig. 2.

Fig. 6b. Dependence of the polarization  $P$  on  $U$  for the case of Fig.6a.

### References

1. H.Uberall, Phys.Rev., 107, 223, 1957.
2. E.V.Sekhpossian, M.L.Ter-Mikaelian, Izvestia Akad. Nauk Arm. SSR, 14, 143, 1961.
3. R.O.Avakian et al., Dokladi Akad.Nauk Arm. SSR,45, 3, 1967.
4. G.Bologna, Nuovo Cimento, 49A, 756, 1967.
5. V.M.Kuznetsov et al., Yadernaya Fizika, 25, 134, 1977.
6. V.M.Epanchintsev et al., Abstract of the Reports of the IX All Union Symposium on Physics of Charged Particle Interaction with Crystals, Moscow, 1978,p.72.
7. R.O.Avakian et al. Scientific Report, EFI-265(58), 1977.
8. G.Diambrini-Polazzi, Rev.Mod.Phys.,40, 611, 1968.
9. H.Olsen, L.C.Maximon, Phys.Rev.,114, 887, 1959.
10. V.N.Bayer,V.M.Katkov,V.S.Fadin,"Izluchenie relyativistskikh elektronov", Atomizdat, 1973.
11. M.L.Ter-Mikaelian "Vliyanie sredi na electromagnitnie protsesi pri visokikh energiakh,Yerevan.Publ.of Academy of Science of Armenia, 1969.
12. B.Neumcke, Phys.Lett., 23, 382, 1966.
13. S.M.Darbinian, K.A.Ispirian,Phys.Lett.,67B, 207, 1977.

The manuscript was received on the 26 of September

С.М.ДАРЬМИНН, К.А.ИСПИРАН  
УГЛОВОЕ РАСПРЕДЕЛЕНИЕ И ПОЛЯРИЗАЦИЯ  
КОГЕРЕНТНОГО ТОРМОЗНОГО ИЗЛУЧЕНИЯ  
(на английском языке)  
Ереванский физический институт

Тех.редактор А.С.Абрамян

Заказ 45I

ВФ-0399I

Тираж 299

Препринт ЕФИ

Подписано к печати 7/ХП-78г.

Формат издания 60x84/16

2.0 уч.изд.л. Ц. 14 к.

Издано Отделом научно-технической информации  
Ереванского физического института, Ереван-36, пер.Маргаряна 2

индекс 3624